Supplement of Biogeosciences, 22, 1651–1671, 2025
https://doi.org/10.5194/bg-22-1651-2025-supplement

Biogeosciences Open Access EGU

Supplement of

Temporal dynamics and environmental controls of carbon dioxide and methane fluxes measured by the eddy covariance method over a boreal river

Aki Vähä et al.

Correspondence to: Aki Vähä (aki.vaha@helsinki.fi)

Introduction

The supporting information contains seven figures and supporting text. The supplement is based on the discussion between the authors and the reviewers during the review process of the manuscript.

Figure S1 shows the distribution of the observed lag times between the vertical wind and the CH_4 mixing ratio.

Figure S2 shows the distribution of the calculated roughness lengths.

Figure S3 shows the time series of the total radiation and the underwater photosynthetically active radiation (PAR). Total radiation was measured at the platform and the weather station. PAR was measured at the platform.

Figure S4 shows the observed quality-controlled sensible heat flux H against $(T_w - T_a)U$.

Figure S5 shows the observed drag coefficient against the wind speed.

Figure S6 shows the observed stability as a function of the time of the day.

Figure S7 shows the quality-controlled CO_2 fluxes as a function of the stability.

Text S1: Lag time

The time delay between the vertical wind and CH_4 mixing ratio was constant throughout the campaign. A histogram of CH_4 lag times is shown in Fig. S1. The distribution of lag times is centred around 70 data points, i.e. 7.0 s.

Text S2: Roughness length

The roughness lengths were calculated from the two adjacent sonic anemometers on the southern side of the platform with the measurement heights z_1 = 1.00 m and z_2 = 1.82 m and wind speeds U_1 and U_2. From the logarithmic wind law, assuming neutral stability and that the measured friction velocities are equal – which they are at a sufficient accuracy –, we can solve

$$z_0 = z_2 \left[\exp\left(\frac{U_2}{U_2 - U_1} \times \log\frac{z_2}{z_1}\right)\right]^{-1}. \quad \text{(S1)}$$

The roughness lengths for cases with accepted fluxes and for the southern wind sector have a median of 0.0145 m and their distribution is shown in Fig. S2.

Following Aubinet et al. (2012) who cite the work by Eugster et al. (2003), the roughness lengths z_0 over small water bodies can be larger than those measured over open ocean. This is caused by increased turbulence due to the vegetation and topography at the shores and that the atmospheric turbulence field over a small water body is not able to equilibrate fully with the water surface over short distances.

Text S3: Radiation

Fig. S3a shows the net radiation

$$rad_{net} = SW_{in} - SW_{out} + LW_{in} - LW_{out}, \quad \text{(S2)}$$

where SW and LW stand for shortwave and longwave radiation, respectively, and the subscripts in and out stand for incoming and outgoing radiation. The radiation was measured at the platform in the river with a CNR4 net radiometer (Kipp & Zonen B.V., Delft, the Netherlands) 0.5 m above the water surface and at the Tähtelä weather station with a CM11 pyranometer (Kipp & Zonen B.V.) 17.5 m above the ground.

Fig. S3b shows the photosynthetically active radiation (PAR) in water at 0.3 m, 0.65 m and 1.00 m depth. The sensors at 0.30 m and 1.00 m were unidirectional underwater quantum sensors Li-192 (LI-COR Environmental, Lincoln, Nebraska, USA). The sensor at 0.65 was the omnidirectional underwater quantum sensor Li-193 (LI-COR).

Text S4: Turbulent exchange coefficients of heat and momentum

In Fig. S4, the sensible heat flux H is shown against the wind speed multiplied with the temperature difference between the water surface and the atmosphere $(T_w - T_a)U$. The points sit on a straight line which indicates that the fluxes originate from the same surface, similarly as in the studies by Nordbo et al. (2011) and Mammarella et al. (2015). The turbulent heat transfer coefficient can be calculated from the slope of the line as

$$C_H = \frac{H}{c_a \rho_a (T_w - T_a) U} \quad \text{(S3)}$$

where c_a is the specific heat capacity of air and ρ_a is the atmospheric density. The turbulent heat transfer coefficient is in our case 1.5×10^{-3}, which fits the theoretical value of $C_H \sim 10^{-3}$ for heat exchange over water (e.g. Wei et al. 2016). The slope of the fitted line is 1.87 which is close to those observed by Nordbo et al. (2011) and Mammarella et al. (2015), whose results were 2.23 and 1.97, respectively.

The drag coefficient (the exchange coefficient of momentum) is calculated as

$$C_D = \left(\frac{u_*}{U}\right)^2 \quad \text{(S4)}$$

where u_* is the friction velocity and U is the mean 30-minute wind speed. The drag coefficients are shown as a function of U in Fig. S5 for the cases with accepted CO_2 fluxes as well as for the cases where the fluxes were not accepted, i.e., when the wind was blowing from land sectors. We only used here the accepted cases from the southern sector because the platform caused additional turbulence to the measurements when the wind was from the north. The drag coefficient over open water is of the order of 10^{-3} (e.g. Guseva et al. 2023) which we also observe, albeit slightly larger than in open ocean. Still, the drag coefficients for the water sector were smaller than when the wind was coming from the land sectors.

Text S5: Stability

The measured stabilities $\zeta = z/L_{MO}$, where z is the height of measurements and $L_{MO}$the Monin–Obukhov length estimated from the eddy covariance measurements, are shown in Fig. S6 as a function of time of day for the cases with accepted fluxes. Stabilities during daytime were mostly between −0.1 and +0.1, which is generally considered near-neutral. In addition, the accepted negative CO_2 fluxes that occurred when the atmosphere above the river was stable accounted for less than 1 % of all the instances with accepted fluxes (Fig. S7).

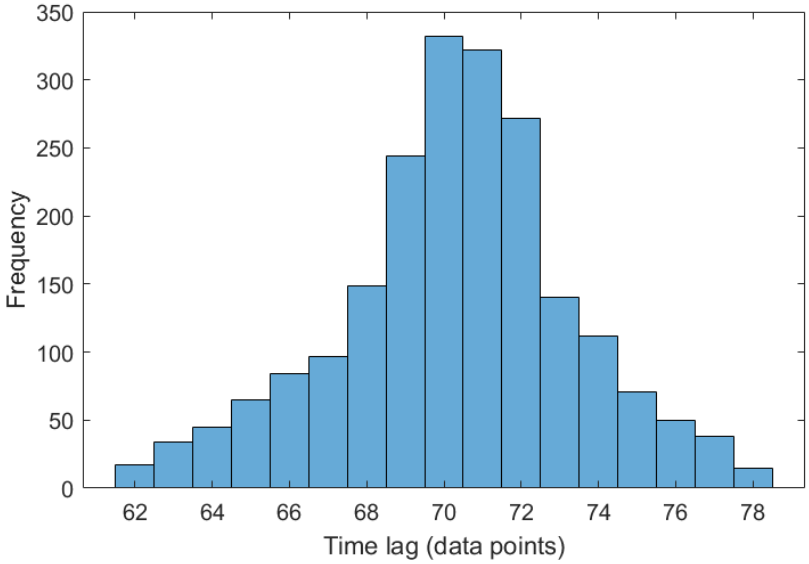

Fig. S1. The distribution of CH_4 lag times in units of data points. The mode corresponds to a lag of 7.0 s.

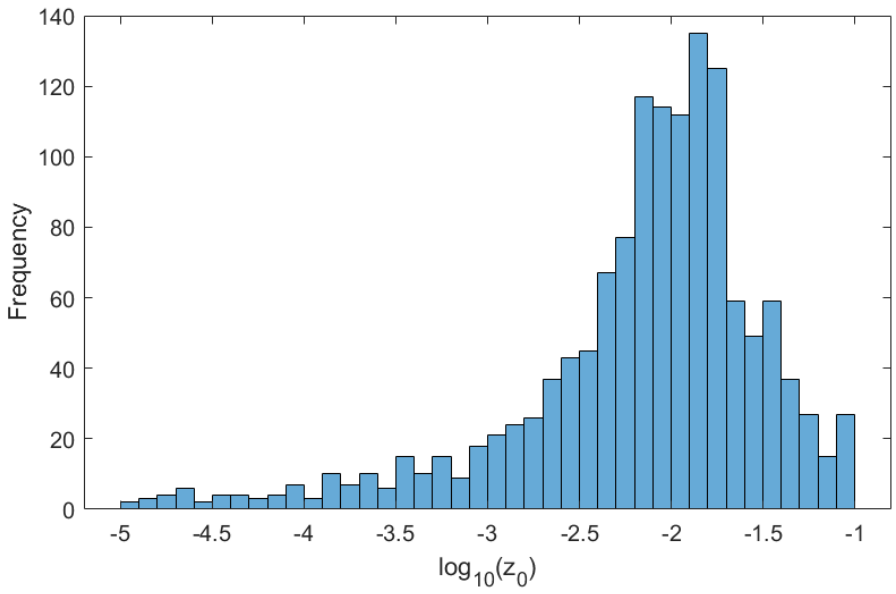

Fig. S2: Distribution of the calculated roughness lengths for cases with accepted fluxes and using only the southern wind sector.

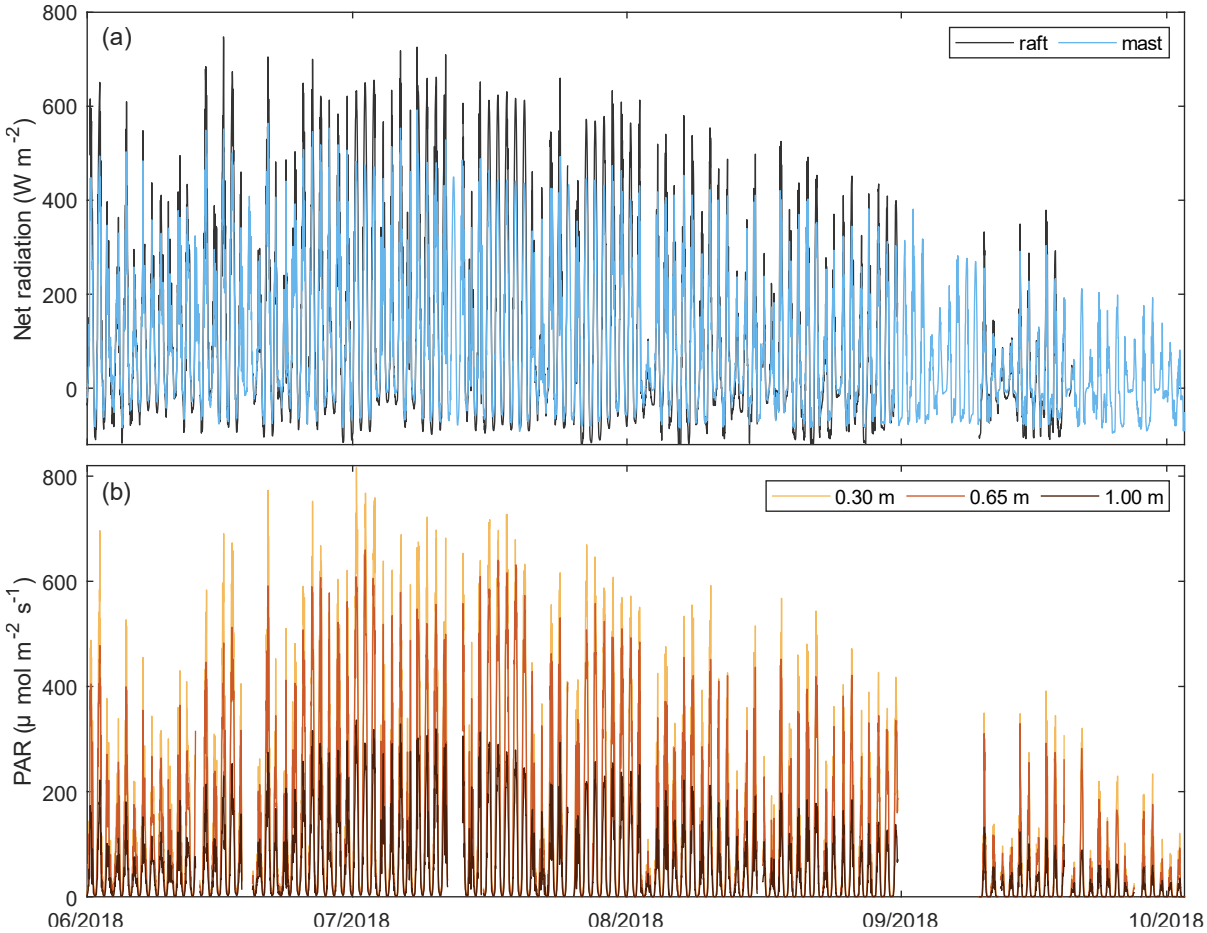

Figure S3. (a) Net radiation in W m^{-2} at the measurement platform (raft) and at the weather station (mast). (b) Photosynthetically active radiation in the water at the depths indicated in the legend in µmol m^{-2} s^{-1}.

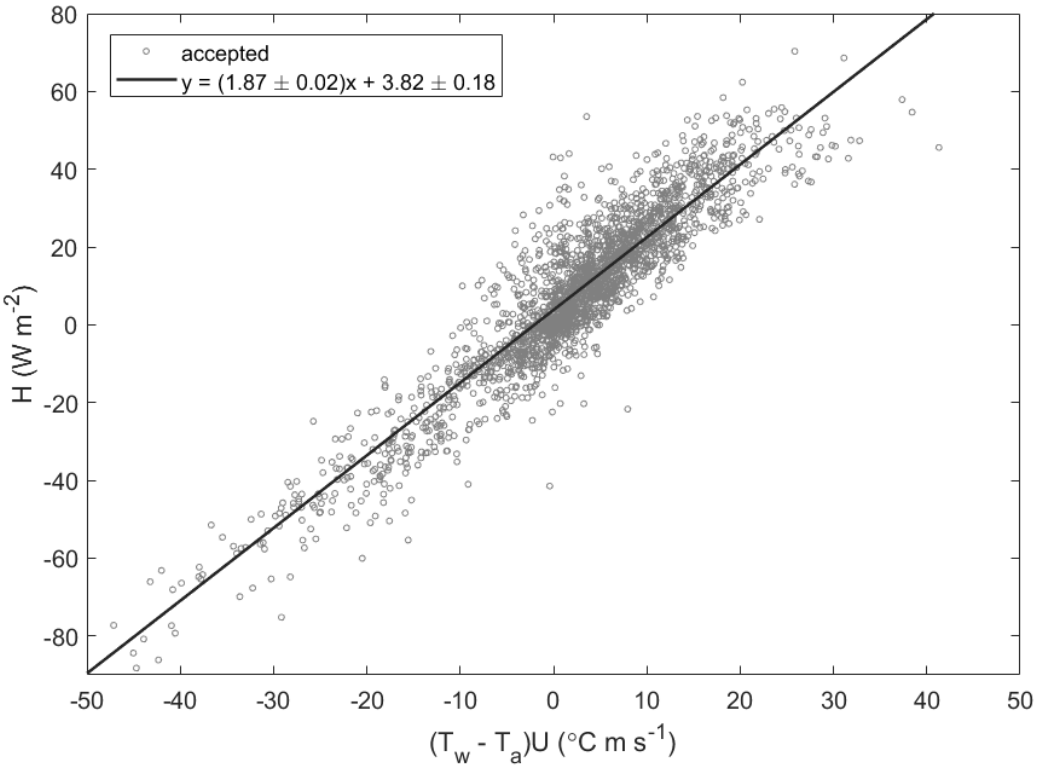

Fig. S4: Sensible heat flux against $(T_w - T_a)U$.

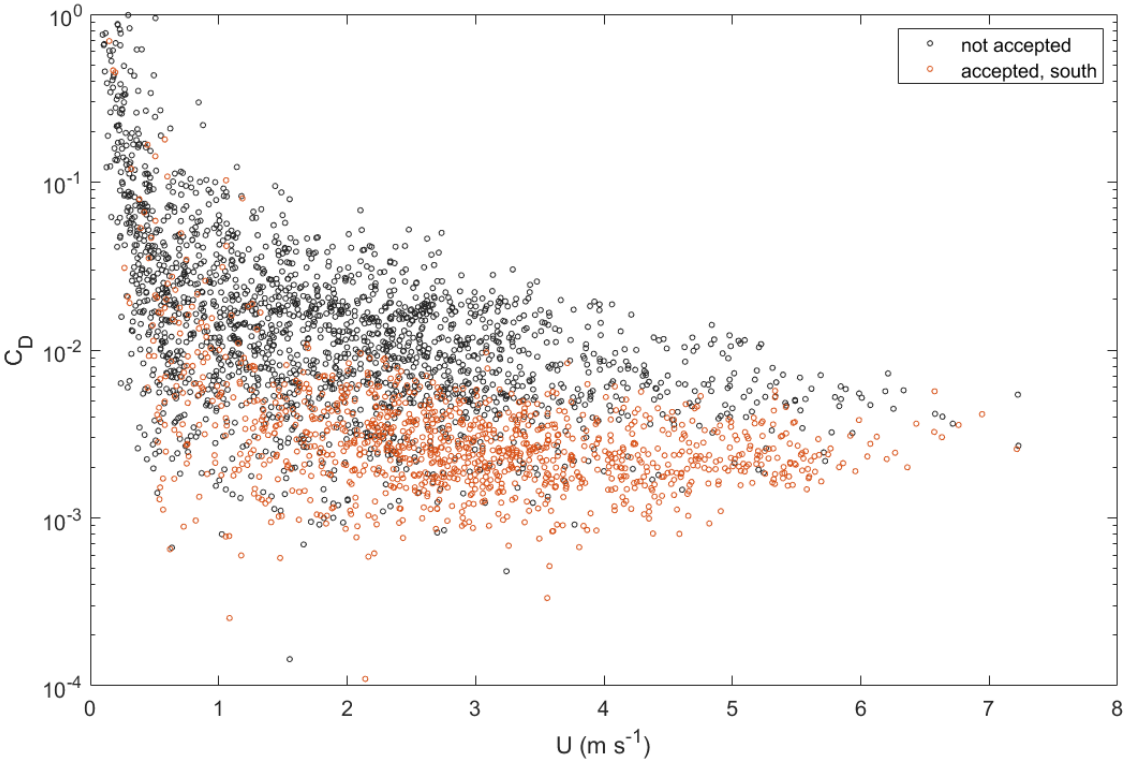

Fig. S5: Drag coefficient against wind speed. Shown here are the drag coefficient from the land sectors ("not accepted") and from the southern wind sector from cases with accepted fluxes.

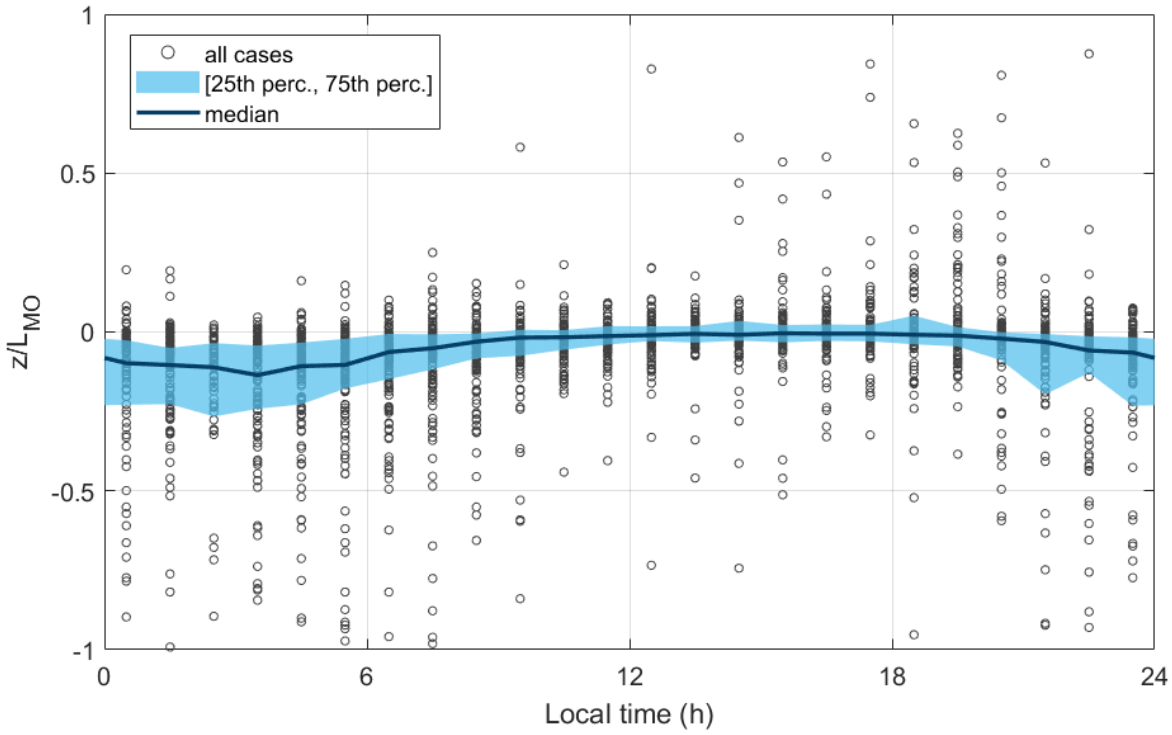

Fig. S6: Stability as a function of time of day for the cases with accepted fluxes. All cases that coincide with the accepted fluxes are plotted with circles. Hourly medians and the area between the 25th and 75th percentiles are plotted with the solid line and shaded area, respectively.

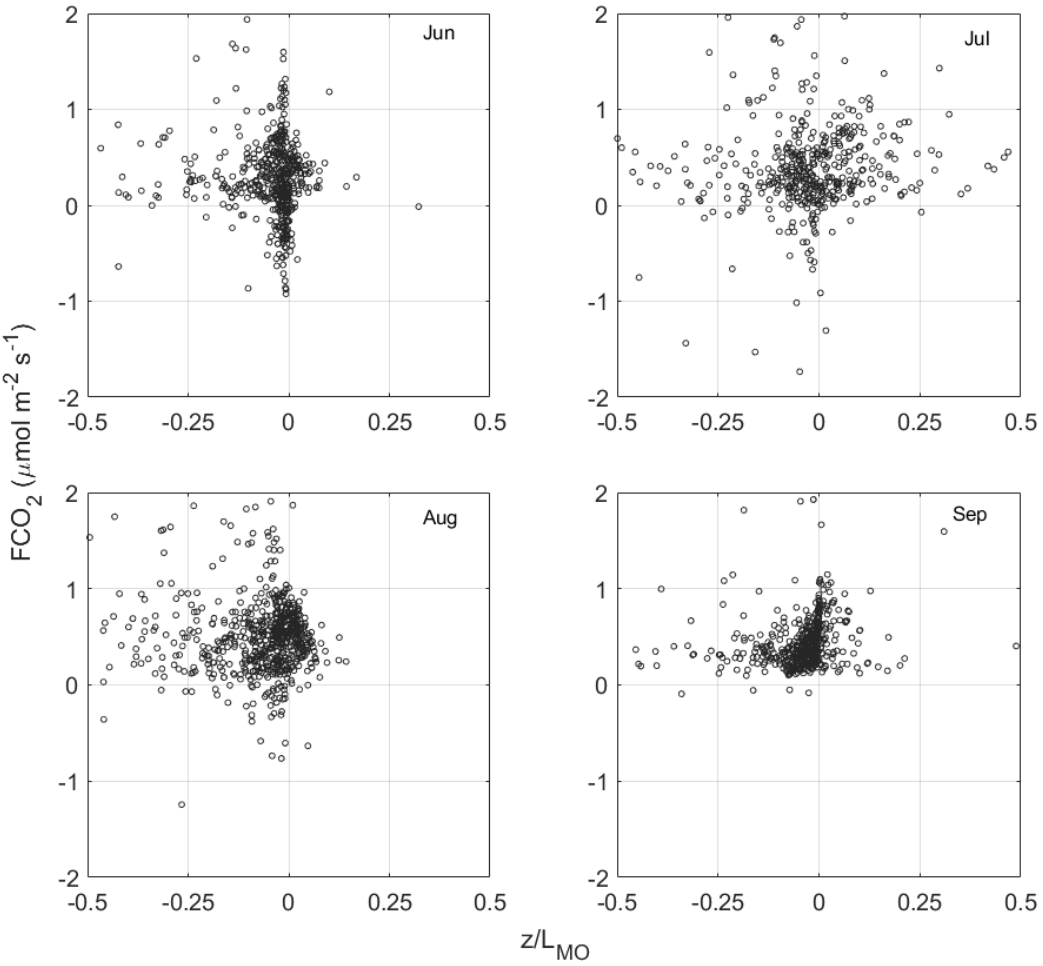

Fig. S7: CO_2 fluxes as a function of stability in different months.

References

Aubinet, M., Vesala, T. and Papale, D. (eds): Eddy covariance, A practical guide to measurement and data analysis, *Springer Science+Business Media B.V.*, Dordrecht, 2012, doi: 10.1007/978-94-007-2351-1.

Eugster, W., Kling, G., Jonas, T., McFadden, J. P., Wüest, A., MacIntyre, S. and Chapin, F. S. III (2003): CO_2 exchange between air and water in an Arctic Alaskan and midlatitude Swiss lake: Importance of convective mixing, *J. Geophys. Res.*, 108, D12, 4362, doi: 10.1029/2002JD002653.

Guseva, S., Armani, F., Desai, A. R., Dias, N. L., Friborg, T., Iwata, H., Jansen, J., Lükő, G., Mammarella, I., Repina, I., Rutgersson, A., Sachs, T., Scholz, K., Spank, U., Stepanenko, V. Torma, P., Vesala, T., Lorke, A. (2023): Bulk transfer coefficients estimated from eddy-covariance measurements over lakes and reservoirs, *J. Geophys. Res. Atmos.*, 128(2), e2022JD037219, doi: 10.1029/2022JD037219.

Mammarella, I., Nordbo, A., Rannik, Ü., Haapanala, S., Levula, J., Laakso, H., Ojala, A., Peltola, O., Heiskanen, J., Pumpanen, J. and Vesala, T. (2015): Carbon dioxide and energy fluxes over a small boreal lake in Southern Finland, *J. Geophys. Res. Biogeosci.*, 120, 1296–1314, doi: 10.1002/2014JG002873.

Nordbo, A., Launiainen, S., Mammarella, I., Leppäranta, M., Huotari, J., Ojala, A. and Vesala, T. (2011): Long-term energy flux measurements and energy balance over a small boreal lake using eddy covariance technique, *J. Geophys. Res.*, 116, D02119, doi: 10.1029/2010JD014542.

Wei, Z., Miyano, A. and Sugita, M (2016): Drag and bulk transfer coefficients over water surfaces in light winds, *Boundary-Layer Meteorol.*, 160, 319–346, doi: 10.1007/s10546-016-0147-8.